Development of all-solid coherent Doppler wind lidar

Xiaopeng Zhu (竹孝鹏), Jiqiao Liu (刘继桥), Decang Bi (毕德仓)
Jun Zhou (周 军), Weifeng Diao (刁伟峰), and Weibiao Chen (陈卫标)*

Shanghai Key Laboratory of All Solid-State Laser and Applied Techniques,
Shanghai Institute of Optics and Fine Mechanics, Chinese Academy of Sciences, Shanghai 201800, China
**Corresponding author: wbchen@mail.shcnc.ac.cn*

Received April 29, 2011; accepted May 19, 2011; posted online July 29, 2011

A 1 064-nm pulsed coherent Doppler lidar (CDL) prototype is developed to measure short range wind speed in the lower altitude troposphere layer. The CDL system adopts an injection–seeded Nd:YAG laser with the pulse duration of 80 ns, single pulse energy of 0.5 mJ, and pulse repetition rate of 200 Hz. Speed calibration experiments are implemented to obtain a speed accuracy of 0.3 m/s using a hard target. Data analysis results show that the CDL system can obtain a line-of-sight wind velocity at a range of 30 to 500 m with the range resolution of 40 m and 38 pulses accumulation.

OCIS codes: 280.3340, 010.0280, 010.3640.
doi: 10.3788/COL201210.012801.

Coherent Doppler lidar (CDL) systems have played a significant role in the fields of wind shear, wake vortices, and clear air turbulence detection[1]. With the development of laser technology, CDL systems at wavelengths of 10.6[2], 1[3,4], 2[5], and 1.5 μm[6,7] have been realized. Compared with 10.6-μm laser sources, CDL systems based on solid-state lasers have attracted more attention due to their small size, light weight, high reliability, and long lifetime[4,8−10]. At a given level of the signal-to-noise ratio (SNR), the lidar at the 1.064-μm wavelength of Nd:YAG offers smaller velocity error and better range resolution than the lidar at longer wavelength[11]. Aerosol backscatter signal of 1.064-μm laser is stronger than those of 1.5- and 2-μm lasers. Thus, a compact all-solid state CDL for wind sensing at a wavelength of 1.064 μm was developed. Both line-of-sight (LOS) wind speed and hard-target calibration experiments were carried out to validate the measurement abilities of the system. The performance of this CDL system can be improved through the receiver subsystem optimization.

The schematic configuration of the CDL system is shown in Fig. 1. The system consists of a pulsed laser, an optical transceiver, and a signal processor. In this system, a 1.064-μm continuous wave (CW) light from the seeder laser source was divided into two beams. One was sent to the balanced receiver and used as the local oscillator (LO) for heterodyne detection. The other part, whose frequency was shifted by an acousto-optical frequency shifter (AOM), was injected into a pulsed laser cavity as a seeder source. The pulsed laser was transmitted to the atmosphere through a quarter waveplate and optical telescope. The backscatter signal from aerosols in the air was received by the same telescope and sent to the balanced receiver through a fiber-port and a 2 × 2 fiber coupler. The reflected signal from the optical lens of the telescope was recorded to derive the intermediate frequency (IF) between the LO and pulsed laser output. The backscatter signal from the aerosols was observed continuously. The radio frequency (RF) signal from the balanced receiver was sent to the signal processor to calculate the Doppler frequency shift (Δf) caused by the LOS speed (V). Detailed explanations of the key components of the system are presented as

$$\Delta f = \frac{2V}{\lambda}. \tag{1}$$

An injection-seeded single frequency Nd:YAG laser with 80-ns pulse duration and 0.5-mJ pulse energy was designed and built[12]. The effective cavity (folded cavity) length of this pulsed laser was approximately 1 m. A 200-mW CW non-planar ring oscillator (NPRO) Nd:YAG laser with a spectral linewidth of 1 kHz (full-width at half-maximum FWHM), was set as the seeder laser. Stable single-longitudinal-mode laser output was obtained by the cavity length controlling method based on a modified ramp-fire technique. The IF between the LO and the pulsed laser output was approximately 62.5 MHz, and the beam quality M^2 factor was 1.4.

The optical transceiver system was collimated in free space. In comparison with 1.5- and 2-μm coherent lidars, the 1.064-μm lidar requires stricter conditions, such as coaxial alignment and optical wavefront quality. Two beam expanding telescopes were inserted to achieve

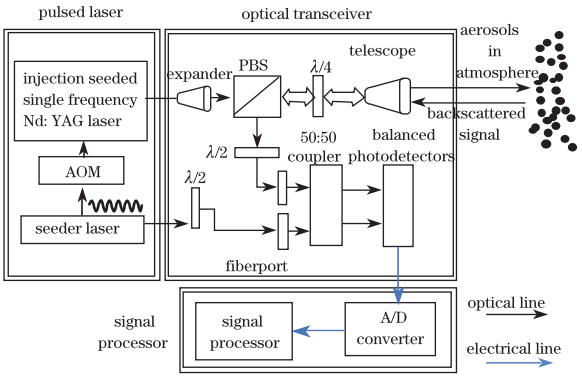

Fig. 1. Schematic diagram of the coherent Doppler lidar. PBS: polarization beam splitter.

the final transmitted beam diameter of approximately 35 mm. The effective diameter of the optical antenna receiver was 55 mm. An optical switch based on polarization beam splitter (PBS) and a quarter waveplate was utilized to separate the transmitting laser and receive backscatter echoes. The collimated laser beam was emitted in a horizontally polarized manner, and thus, fully went through the PBS. After passing through the quarter waveplate, the backscattered light was reflected by the PBS and coupled into the fiber by a fiber-port with a specially designed focused lens. The backscatter signal was mixed with the local oscillator laser in a polarization-maintaining (PM) single-mode 2 × 2 fiber coupler with a coupling ratio of 50:50. Heterodyne mixed signal was detected by a balanced photodetector (PDB130C, Thorlabs). According to the parameters of the photodetector, the power of the LO was set to 0.5 mW, which could be adjusted through the fiber-port.

The output RF signal from the balanced detectors was sampled by an 8-bit A/D converter at a sampling rate of 1 GS/s. The signals were divided into several bins at a 40-m range resolution. The power spectrum for each range bin was obtained by fast Fourier transformation (FFT) algorithm. By increasing the number of points for FFT, the frequency resolution could be improved considerably. A total of 2 048 points was achieved by zero padding method to obtain a 0.49-MHz frequency resolution. A Hanning window was added to reduce the spectral leakage. Incoherent spectrum accumulations were processed to increase SNR and improve velocity estimation accuracy at each range bin. The LOS velocity of each range bin was estimated by searching the frequency that corresponds with the peak of the signal power spectrum density (PSD).

The speed measurement accuracy of the CDL system was important for applications. Thus, experiments of hard-target calibration at different speeds were carried out to evaluate the measurement accuracy. A rotary disk wheel acting as a hard target and driven by a stepper motor, was placed 40-m away. The transmitted laser of the CDL was attenuated and focused on the edge of the disk wheel through a long focal length converging lens. The speed of the edge of the wheel can be adjusted from –6.85 to +6.85 m/s by a computer, which was connected to the motor. The received heterodyne mixing signals are shown in Fig. 2(a). The first group of echoes was scattered by the telescope optics. The second group of echoes was from the rotating wheel, and the speed of the edge of the wheel was –6.85 m/s. The PSDs of the two echoes are shown in Fig. 2(b).

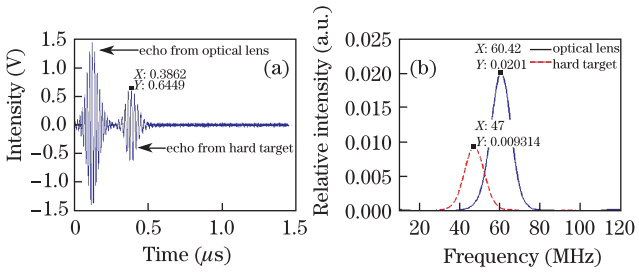

Fig. 2. Heterodyne mixing signal and PSD from hard-target speed calibration experiments. (a) Heterodyne mixing signal; (b) relative PSD of mixing signal.

The frequencies corresponding to the peak of the PSD were 60.42 and 47 MHz, respectively. Hence, the Doppler frequency shift was –13.42 MHz, and the speed of the edge of the wheel was –7.14 m/s. Thus, the speed error was 0.29 m/s. A series of experimental comparisons between the detected target speed and the actual speed with different rotator speeds was performed. The results are shown in Fig. 3. The *R*-square of the linear fit was 0.9985. The variance of speed measurement was approximately 0.3 m/s, which demonstrates excellent speed measurement with high accuracy.

Preliminary experiments were executed to detect the atmosphere LOS wind speed at the range of 30 to 500 m with a 0° elevation angle. In the direction of the transmitted laser, a building was located 570-m away, which was also used to estimate the IF between the LO and pulsed laser output. The heterodyne signal from the balanced detector is shown in Fig. 4. The signal at approximately 3 μs was reflected by the optical lens of the telescope, and the signal at approximately 6.8 μs was reflected by the building. The signals between 3 and 6.8 μs were scattered by the aerosols in the atmosphere. The accumulated PSDs from 38 pulses are shown in Fig. 5. The Doppler frequency shifts could be acquired by identifying the frequency that corresponds with the peak of PSDs. The LOS wind velocity measurements at a range of 30 to 500 m with the 40-m range resolution are shown in Fig. 6. As an option, the adjacent bins could be averaged to smooth the wind measurements.

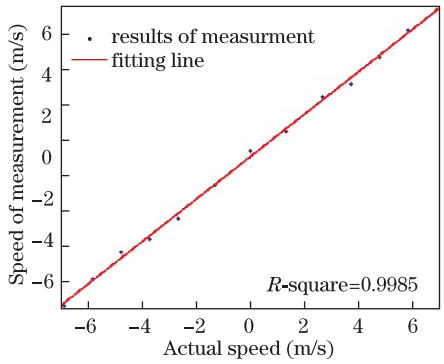

Fig. 3. Comparison between the detected target speed and actual speed. *R*-square 0.9985 of the linear fit is proven.

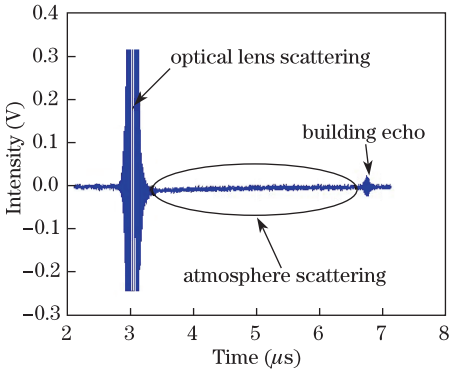

Fig. 4. Heterodyne mixing signal from the balanced receiver.

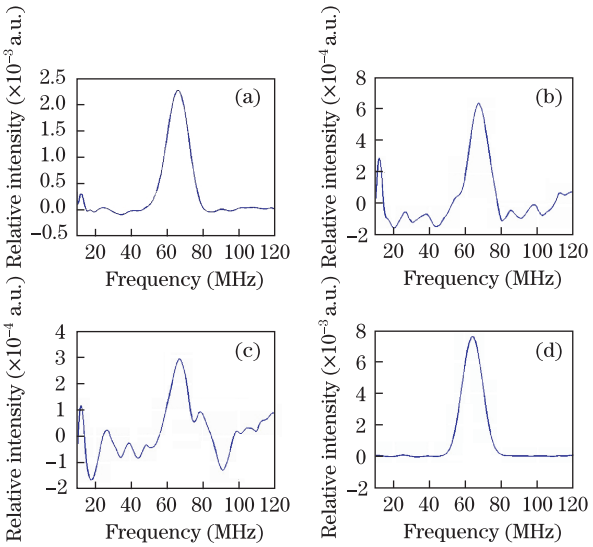

Fig. 5. PSD of 38 pulse accumulations. PSD of signal at (a) 90, (b) 185, and (c) 330 m. (d) PSD of signal reflected by building (at 570 m).

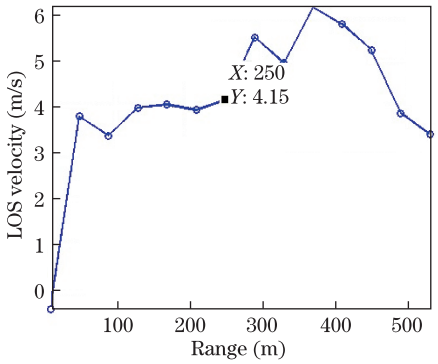

Fig. 6. LOS wind velocity measurement at a range of 30 to 500 m with a 0° elevation angle.

In conclusion, a compact all-solid pulsed CDL system for wind speed profile sensing is developed. A speed calibration experiment is carried out to demonstrate the speed measurement accuracy of 0.3 m/s. Through PSD incoherent accumulation from 38 pulses, atmosphere LOS wind velocities within the range of 30 to 500 m are measured with the 40-m range resolution. The preliminary results of the CDL system is obtained, and the system is performance will be improved by optimizing the system parameters and signal processing algorithm.

This work was supported by the National Natural Science Foundation of China under Grant No. 60908036.

References

1. C. M. Shun and P. W. Chan, J. Atmos. Ocean. Technol. **25,** 637 (2008).
2. F. F. H. Jr. Freeman, R. M. Huffaker, R. M. Hardesty, M. E. Jackson, T. R. Lawrence, M. J. Post, R. A. Richter, and B. F. Weber, Appl. Opt. **23,** 2503 (1984).
3. T. J. Kane, W. J. Kozlovsky, R. L. Byer, and C. E. Byvik, Opt. Lett. **12,** 239 (1987).
4. S. W. Henderson, R. M. Huffaker, M. J. Kavaya, C. P. Hale, J. R. Magee, and C. L. E. Myers, Proc. SPIE **1222,** 118 (1990).
5. G. J. Koch, J. Y. Beyon, B. W. Barnes, M. Petros, J. Yu, F. Amzajerdian, M. J. Kavaya, and U. N. Singh, Opt. Eng. **46,** 116201 (2007).
6. S. Kameyama, T. Ando, K. Asaka, Y. Hirano, and S. Wadaka, Appl. Opt. **46,** 1953 (2007).
7. F. Yang, Y. He, J. Shang, and W. Chen, Chin. Opt. Lett. **8,** 713 (2010).
8. J. G. Hawley, R. Targ, R. Bruner, S. W. Henderson, C. P. Hale, S. Vetorino, R. W. Lee, S. Harper, and T. Khan, Proc. SPIE **1694,** 110 (1992).
9. C. Liu, Y. Qi, Y. Ding, J. Zhou, J. Dong, Y. Wei, and Q. Lou, Chin. Opt. Lett. **9,** 031402 (2011).
10. J. Wang, J. Zhou, H. Zang, X. Zhu, and W. Chen, Chin. Opt. Lett. **8,** 670 (2010).
11. T. J. Kane, B. Zhou, and R. L. Byer, Appl. Opt. **23,** 2477 (1984).
12. J. Zhou, H. Zang, D. Liu, J. Bi, J. Liu, J. Wang, X. Zhu, and W. Chen, in *Proceedings of CLEO/PACIFIC RIM* 1–2 (2009).